Low-complexity noise-resilient recovery of phase and amplitude from defocused intensity images

Zhong Jingshan[1], **Justin Dauwels**[1], **Manuel A. Vázquez**[2], **Laura Waller**[3]

[1] *Nanyang Technological University, School of Electrical and Electronic Engineering, Singapore 639798*
[2] *Universidad Carlos III de Madrid, Depto. de Teoría de la Señal y Comunicaciones, Madrid, Spain.*
[3] *Princeton University, Department of Electrical Engineering, Princeton, NJ 08544 US*

zhongjingshan@hotmail.com, jdauwels@ntu.edu.sg

Abstract: A low-complexity augmented Kalman filter is proposed to efficiently recover the phase from a series of noisy intensity images. The proposed method is robust to noise, has low complexity, and may enable real-time phase recovery.

OCIS codes: 100.5070, 100.3010.

1. Introduction

When coherent light propagates through an object, its amplitude and phase change after interacting with the object. The phase perturbations reveal important information about the object, for example, refractive index, humidity, or pressure. Consequently, phase imaging has many important applications in areas like biology and surface profiling. As phase cannot be measured directly, it needs to be reconstructed computationally. This "phase problem" of optical imaging has been studied for many years, but only recently has it been investigated from the viewpoint of statistical inference [1–3], where experimental noise in the images is modeled explicitly.

Standard methods for recovering phase involve complicated interferometric setups, so there is a significant experimental advantage to methods considered here, which reconstruct the phase from intensity images captured at various distances along the optical axis. In [2] an extended Kalman filter was applied to infer the phase from noisy intensity images. However, the memory requirements and the long computation time are impractical for real applications. In [3] an approximate Kalman filter was proposed that alleviates those issues, without jeopardizing the reconstruction accuracy. That method is iterative: it needs to cycle through the set of intensity images repeatedly, yielding more accurate phase reconstruction after each cycle. On the other hand, the computational complexity increases with each cycle.

The algorithm proposed here does not require iterations, and is more efficient than the algorithm of [3], yet it achieves even better phase reconstruction than the methods of [2] and [3]. As in [2], the proposed algorithm is derived from an augmented state space representation, to improve the robustness to noise. We make similar approximations as in [3] (where the state space was *not* augmented), and introduce a few additional assumptions to simplify the Kalman filter update equations [2], eventually resulting in a low-complexity noise-robust phase reconstruction algorithm.

2. Problem Description and State Space Model of the Optical Field

We aim at estimating the 2D complex-field $A(x,y,z_0)$ at the focal plane z_0, from a sequence of noisy intensity images $I(x,y,z)$ captured at various distance $z_0, z_1, z_2, \ldots, z_N$. Propagation is modeled by the homogeneous paraxial wave equation:

$$\frac{\partial A(x,y,z)}{\partial z} = \frac{i\lambda}{4\pi}\nabla_{\perp}^{2} A(x,y,z), \tag{1}$$

where λ is the wavelength of the illumination, and $\nabla_{\perp}$ is the gradient operator in the lateral (x,y) dimensions only. The noisy measurements $I(x,y,z)$ usually adhere to a (continuous) Poisson distribution:

$$p[I(x,y,z)|A(x,y,z)] = e^{-\gamma|A(x,y,z)|^2}\frac{(\gamma|A(x,y,z)|^2)^{I(x,y,z)}}{I(x,y,z)!}, \tag{2}$$

where γ is the photon count detected by the camera. The measurement at each pixel $I(x,y,z)$ is assumed statistically independent of any other pixel (conditioned on the optical field $A(x,y,z)$).

We can discretize the optical field $A(x,y,z)$ as a raster-scanned complex column vector $\mathbf{a}_n$, and similarly discretize the measurement $I(x,y,z)$ as column vector $\mathbf{I}_n$. We denote by $b(u,v,z)$ the 2-D Fourier transform of $A(x,y,z)$. The column vector $\mathbf{b}_n$ is again raster-scanned from $b(u,v,z)$, and hence can be expressed as $\mathbf{b}_n = \mathbf{K}\mathbf{a}_n$, where $\mathbf{K}$ is the discrete Fourier transform matrix.
We can define the propagation matrix at z_n as [4]:

$$\mathbf{H}_n = \mathrm{diag}\Big(\exp\Big[-i\lambda\pi\Big(\frac{u_1^2}{L_x^2}+\frac{v_1^2}{L_y^2}\Big)\Delta_n z\Big],\dots,\exp\Big[-i\lambda\pi\Big(\frac{u_M^2}{L_x^2}+\frac{v_N^2}{L_y^2}\Big)\Delta_n z\Big]\Big), \tag{3}$$

where L_x and L_y are the width and height of the image.

We approximate the Poisson observation model (2) with a Gaussian distribution of same mean and covariance. As in [2], we consider a state space representation with augmented state:

$$state: \begin{bmatrix}\mathbf{b}_n\\ \mathbf{b}_n^*\end{bmatrix} = \begin{bmatrix}\mathbf{H}_n & 0\\ 0 & \mathbf{H}_n^*\end{bmatrix}\begin{bmatrix}\mathbf{b}_{n-1}\\ \mathbf{b}_{n-1}^*\end{bmatrix} \tag{4}$$

$$observation: \mathbf{I}_n = \begin{bmatrix}\mathbf{J}(\mathbf{b}_n) & \mathbf{J}^*(\mathbf{b}_n)\end{bmatrix}\begin{bmatrix}\mathbf{b}_n\\ \mathbf{b}_n^*\end{bmatrix} + \mathbf{v}, \text{ with } \mathbf{v}\sim\mathscr{N}(0,\mathbf{R}(\mathbf{b}_n)), \tag{5}$$

where

$$\mathbf{R} = \gamma\,\mathrm{diag}(\mathbf{a}_n^*)\mathrm{diag}(\mathbf{a}_n); \mathbf{J}(\mathbf{b}_n) = \frac{1}{2}\gamma\,\mathrm{diag}(\mathbf{K}^T\mathbf{b}_n^*)\mathbf{K}^H. \tag{6}$$

The augmented state (4) introduces redundancy, which helps to improve the resilience to noise.

3. State Estimation by Low-Complexity Kalman Filtering

Table 1 summarizes the augmented Kalman filter of [2]. The storage requirement scales as N^2, where N is the number of pixels. The computational complexity scales as $\mathscr{O}(N^3N_z)$, where N_z is the number of intensity images. Due to the high complexity, the algorithm is impractical for real-time applications. Therefore, we impose constraints on the covariance matrices $\mathbf{S}_0^Q$ and $\mathbf{S}_0^P$, and make several assumptions, resulting in a low-complexity algorithm with reduced storage requirement. Specifically, in the proposed algorithm, $\mathbf{S}_0^Q$ and $\mathbf{S}_0^P$ are diagonal matrices. Consequently, the storage requirement scales linearly with N. The overall computational complexity is reduced to $\mathscr{O}(N_zN\log(N))$.

Table 1. Augmented Kalman filter of [2] for inferring the optical field.

(1) Initialize $\mathbf{b}_0$, $\mathbf{S}_0^Q$, and $\mathbf{S}_0^P$.

(2) Prediction: $\widehat{\mathbf{b}_n} = \mathbf{H}\mathbf{b}_{n-1}$, $\widehat{\mathbf{S}_n^Q} = \mathbf{H}\mathbf{S}_{n-1}^Q\mathbf{H}^H$, and $\widehat{\mathbf{S}_n^P} = \mathbf{H}\mathbf{S}_{n-1}^P\mathbf{H}$.

(3) Update:

$$\widehat{\mathbf{a}_n} = \mathbf{K}^H\widehat{\mathbf{b}_n} \tag{7}$$

$$\mathbf{S}_n^Q = \widehat{\mathbf{S}_n^Q} - (\widehat{\mathbf{S}_n^Q}\mathbf{J}^H + \widehat{\mathbf{S}_n^P}\mathbf{J}^T)(\mathbf{J}\widehat{\mathbf{S}_n^Q}\mathbf{J}^H + \mathbf{J}\widehat{\mathbf{S}_n^P}\mathbf{J}^T + \mathbf{J}^*(\widehat{\mathbf{S}_n^Q})^*\mathbf{J}^T + \mathbf{J}^*(\widehat{\mathbf{S}_n^P})^*\mathbf{J}^H + \mathbf{R})^{-1}(\mathbf{J}\widehat{\mathbf{S}_n^Q} + \mathbf{J}^*(\widehat{\mathbf{S}_n^P})^*) \tag{8}$$

$$\mathbf{S}_n^P = \widehat{\mathbf{S}_n^P} - (\widehat{\mathbf{S}_n^Q}\mathbf{J}^H + \widehat{\mathbf{S}_n^P}\mathbf{J}^T)(\mathbf{J}\widehat{\mathbf{S}_n^Q}\mathbf{J}^H + \mathbf{J}\widehat{\mathbf{S}_n^P}\mathbf{J}^T + \mathbf{J}^*(\widehat{\mathbf{S}_n^Q})^*\mathbf{J}^T + \mathbf{J}^*(\widehat{\mathbf{S}_n^P})^*\mathbf{J}^H + \mathbf{R})^{-1}(\mathbf{J}\widehat{\mathbf{S}_n^P} + \mathbf{J}^*(\widehat{\mathbf{S}_n^Q})^*) \tag{9}$$

$$\mathbf{b}_n = \widehat{\mathbf{b}_n} + (\mathbf{S}_n^Q\mathbf{J}^H + \mathbf{S}_n^P\mathbf{J}^T)\mathbf{R}^{-1}(\mathbf{I}_n - \gamma|\mathbf{a}_n|^2). \tag{10}$$

4. Numerical Results

4.1. Data Set 1 (Synthetic data)

Data Set 1 consists of 100 images of size 100×100 pixels artificially generated to simulate a complex field propagating from focus in 0.5 μm steps over a distance of 50 μm with illumination wavelength of 532 nm. Pixels are corrupted by Poisson noise so that, on average, each pixel detects $\gamma = 0.998$ photons.

Table 2 and Fig. 1(a) summarize the results of different methods for the Data Set 1. The extended Kalman filter [2] has a computational complexity of $\mathscr{O}(N_zN^3)$. In order to reduce the computation and storage burden, the images are divided in to separate blocks of size 50×50, but the extended Kalman filter still takes 13563 seconds to process the 100 images. The computational complexity of the iterative method of [3] is $\mathscr{O}(N_{\mathrm{it}}N_zN\log N)$ with N_{it} the number of iterations, and it takes 0.30 seconds per iteration to process all images. We have applied 50 iterations in total, and

Table 2. Comparison of different methods.

	Complexity	Time[s]	Storage	Intensity error	Phase error[radian]
Extended Kalman filter [2]	$\mathcal{O}(N_z N^3)$	13563(in block)	$\mathcal{O}(N^2)$	0.0091	0.0139
Iterative Kalman filter [3]	$\mathcal{O}(N_{\text{it}} N_z N \log N)$	0.30/iteration	$\mathcal{O}(N)$	0.0079	0.0166
Efficient augmented Kalman filter	$\mathcal{O}(\mathbf{N_z N \log N})$	**0.40**	$\mathcal{O}(\mathbf{N})$	**0.0071**	**0.0143**

hence the total computation time was 15s. On the other hand, the computational complexity of the proposed method is $\mathcal{O}(N_z N \log N)$, and it takes 0.40 seconds to process all images. The phase and intensity error of the proposed method is lower than that of the iterative filter of [3].

As can be seen from Fig. 1(a), the images recovered by the extended Kalman filter [2] exhibit block artifacts. The images recovered by the iterative filter of [3] show traces of phase in the intensity images and vice versa. In contrast, the intensity and phase image reconstructed by the proposed method contain virtually no artifacts, and the phase image has stronger contrast.

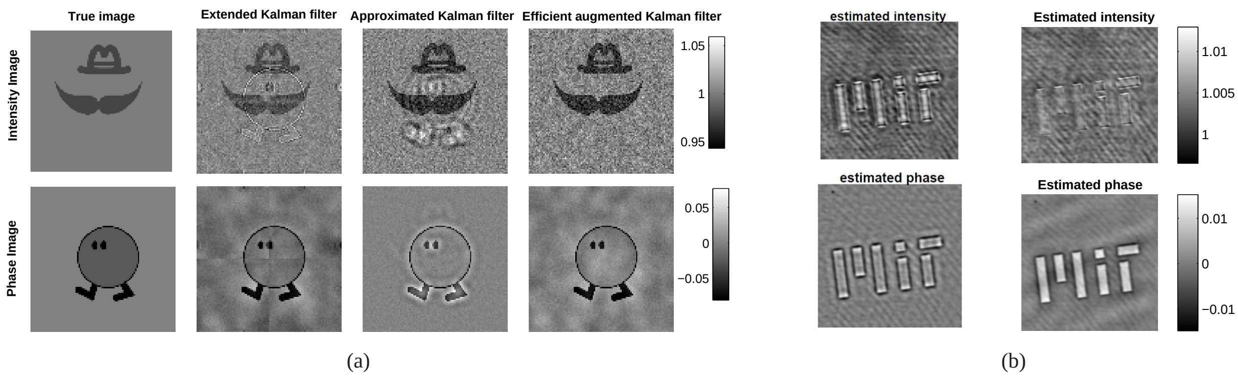

Fig. 1. (a) Recovered intensity and phase image from synthetic Data Set 1 by extended Kalman filter of [2], iterative Kalman filter of [3], and the proposed method. (b) Recovered intensity and phase image from experimental Data Set 2 by iterative Kalman filter of [3] (left) and the proposed method (right).

4.2. Data Set 2 (Experimental data)

Data Set 2 is comprised of 50 images of size 150×150 pixels acquired by a microscope. The wavelength was again 532 nm, and the defocused intensity images were captured by moving the camera axially with a step size of 2 μm over a distance of 100 μm. The test phase object was electron beam etched into PMMA substrate. Fig. 1(b) shows the estimated intensity and phase image for the iterative Kalman filter of [3] and the proposed method. As for Data Set 1, the intensity and phase image inferred by the proposed method contain less artifacts, and the phase image has stronger contrast.

5. Conclusion

The proposed statistical inference algorithm can efficiently recover phase and amplitude from a series of noisy defocused images. It is recursive, and may enable real-time applications. Our method may also find use in phase imaging beyond optical wavelengths (for example, X-ray or neutron imaging), where high-quality images are difficult to obtain and noise is significant and unavoidable.

References

1. R. Paxman, T. Schulz, and J. Fienup. "Joint estimation of object and aberrations by using phase diversity," *J. Opt. Soc. Am. A*, 9(7):1072–1085, 1992.
2. L. Waller, M. Tsang, S. Ponda, and G. Barbastathis. "Complex-field estimation by Kalman filtering," *Opt. Express*, 19(3):2805–2815, 2011.
3. Zhong Jingshan, J. Dauwels, M. A. Vázquez, L. Waller, "Efficient Gaussian Inference Algorithms for Phase Imaging", *Proc. IEEE ICASSP 2012*, Mar 25–30, 2012, Kyoto, Japan.
4. J. Goodman, *Introduction to Fourier Optics*, McGraw-Hill.